Available online at www.sciencedirect.com
ScienceDirect
Cement and Concrete Research 36 (2006) 2074–2085
Cement and Concrete Research

Characterizing Enhanced Porosity Concrete using electrical impedance to predict acoustic and hydraulic performance

Narayanan Neithalath [a], Jason Weiss [b,*], Jan Olek [b]

[a] Department of Civil and Env. Engineering, Clarkson University, Potsdam, NY 13699, USA
[b] School of Civil Engineering, Purdue University, West Lafayette, IN 47907, USA

Received 14 August 2006; accepted 2 September 2006

Abstract

Enhanced Porosity Concrete (EPC) is manufactured by gap grading coarse aggregates to create interconnected porosity in the system. The porosity and physical features of the pore network are characterized in this paper using Electrical Impedance Spectroscopy (EIS). Porosity alone was found to be an inaccurate indicator of the electrical conductivity of the sample. While several studies have shown that a conventional form of Archie's law can describe porous systems, it was observed that Archie's law did not completely describe the electrical conductivity of the EPC system. Therefore, a modified version of Archie's law was used that incorporated the matrix conductivity, which described the system more accurately than the conventional form. The pore connectivity factor determined using EIS is found to be linearly related to the acoustic absorption of the material. Similarly, conductivity results determined from EIS were used with total porosity to compute the hydraulic connectivity factor. This factor was related to intrinsic permeability calculated from hydraulic conductivity (measured using a falling head permeameter). Based on these studies, it appears that a single electrical impedance test could provide information for the design, quality control/quality assurance, and utilization of EPC.

Keywords: Characterization (B); Electrical properties (C); Permeability (C); Porosity; Enhanced Porosity Concrete

1. Introduction

The noise resulting from the interaction between tire and pavement is increasingly being recognized as a significant environmental issue. The use of Enhanced Porosity Concrete (EPC) as an overlay on conventional concrete pavements has been suggested as one possible solution to this problem [1,2]. EPC is proportioned by gap grading the coarse aggregates and either eliminating or minimizing the sand volume in the matrix to develop a network of interconnected pores within the material. The noise reduction that results from the use of this material is believed to occur due to the combined effect of lower noise generation and increased sound absorption. The porous surface is believed to minimize air pumping (the pumping of air in and out of the tread blocks of the tire, which is currently thought to be one of the primary noise generation mechanisms), thereby reducing the noise generation while the pores inside the material also absorb sound energy through internal friction [3]. The key factors that dictate the efficiency of EPC in absorbing sound are the porosity that can be accessed by the sound waves, pore size, pore aperture size, and thickness of porous layer. For EPC to be effective in sound absorption, it has been recommended that 15–25% accessible porosity (by total volume of the material) is needed [1,2,4,5].

In addition to sound absorption, EPC also offer other potential advantages including rapid drainage of water through the interconnected voids which minimizes wet weather spray and reduces glare [6]. The percolation of water through the porous concrete layer recharges ground water and conserves water resources. As a result, porous surfaces in parking lots are believed to help infiltration and cleansing of storm water, thus reducing the adverse environmental impact of impervious parking areas [7].

It is evident from the previous discussion that the total porosity and pore structure play a significant role in the overall performance of EPC with respect to acoustic absorption and

* Corresponding author. Tel.: +1 765 494 2215; fax: +1 765 496 1364.
E-mail address: wjweiss@ecn.purdue.edu (J. Weiss).

0008-8846/$ - see front matter © 2006 Elsevier Ltd. All rights reserved.
doi:10.1016/j.cemconres.2006.09.001

water drainage. Therefore, it is essential that methods to characterize the pore structure of EPC are developed.

2. Research significance

The objective of this paper is to develop test methods to assess the physical features of the pore system of EPC. The electrical conductivity of EPC was measured and used to describe the porosity and pore connectivity using a modified form of Archie's equation that considers two conducting phases [8]. A falling head permeameter was used to quantify the hydraulic conductivity. Results from the falling head permeameter were described using the Kozeny–Carman equation [9,10]. An impedance tube was used to determine the acoustic absorption of EPC. Finally, this paper develops a relationship between measured characteristics (i.e., pore volume and electrical conductivity) and the pore structure (connectivity) for use in the prediction of acoustic absorption and hydraulic conductivity (i.e., permeability) of EPC.

3. Experimental program

The materials, mixtures, and test methods used in this study are described in this section. Specifically, the determination of porosity by a simple water saturation method, electrical conductivity by impedance spectroscopy, hydraulic conductivity by a falling head permeameter, and acoustic absorption by impedance tube are described.

3.1. EPC mixtures

The mixture proportions used in this study (Table 1) were adopted from a larger experimental program that has been designed to determine the mechanical and acoustic properties of EPC [5]. Mixtures were made using single sized aggregates (limestone aggregates with a specific gravity 2.72) — #8 (2.36–4.75 mm), #4 (4.75–9.5 mm), and 3/8″ (9.5–12.5 mm), as well as the binary blends of these aggregate sizes (i.e., by replacing 25, 50, and 75% by weight of the larger aggregates with smaller sized aggregates). One series of mixtures had 2.5%, 5%, and 7.5% of #4 aggregates replaced by river sand. The water–cement ratio (w/c) of all mixtures was kept constant at 0.33. The mixtures were prepared using a laboratory mixer in accordance with ASTM C 192-00 [11], cast in 150 × 150 × 700 mm molds, and consolidated using external vibration. Cylinders (95 mm diameter) were cored from the above beam specimens and used to study acoustical, electrical, and hydraulic properties.

3.2. Measurement of porosity

Because of the presence of large sized interconnected pores in the EPC system (2–4 mm, as compared to the micrometer sized pores in conventional concrete), the following procedure was adopted to determine the porosity. The cylindrical specimens (95 mm in diameter and 150 mm long) that were cored from beams were immersed in water for 24 h to saturate the pores in the matrix with water. After this period, the sample was removed from water and allowed to achieve a saturated surface dried (SSD) condition. The sample was then enclosed in a latex membrane and the bottom of the cylinder was sealed to a stainless steel plate using silicone sealant. The combined mass of the sample, latex membrane, and the steel plate (M_1) was measured. Water was added to the top of the sample until it was filled, which indicated that all the interconnected pores were saturated. The mass of the system filled with water was then taken (M_2). The difference between the masses ($\Delta M = (M_2 - M_1)$) gives the mass of the water in the pores. This mass was converted into a volume, and expressed as a percentage of the total volume of the specimen to provide an indication of the total porosity. Table 1 shows the porosities of various mixtures determined by the procedure stated above, which have been used for all the analyses in this paper. In addition to this procedure, porosity was previously determined using an image analysis procedure. In this procedure, EPC specimen was impregnated with a low viscosity epoxy, and sectioned at different depths. The surface of each section was scanned, and an image analysis procedure was employed to distinguish between the accessible and inaccessible (to the acoustic waves) porosities [5]. The values of porosities determined by this method are also given in Table 1. It can be seen that a reasonable

Table 1
Mixture proportions and porosity

Mixture ID	% 3/8″ aggregates	% #4 aggregates	% #8 aggregates	% Fine aggregate (sand)	Water–cement ratio (w/c)	Porosity (volume method)	Porosity (image analysis method)
100–#8	0	0	100	0	0.33	0.207	0.214
75-#8–25-#4	0	25	75	0	0.33	0.208	0.305
50-#8–50-#4	0	50	50	0	0.33	0.247	0.260
25-#8–75-#4	0	75	25	0	0.33	0.225	0.276
100–#4	0	100	0	0	0.33	0.206	0.203
75-#8–25-3/8	25	0	75	0	0.33	0.225	0.219
50-#8–50-3/8	50	0	50	0	0.33	0.190	0.151
25-#8–75-3/8	75	0	25	0	0.33	0.174	0.244
100–3/8	100	0	0	0	0.33	0.193	0.237
50-#4–50-3/8	50	50	0	0	0.33	0.264	0.303
97.5-#4– 2.5 sand	0	97.5	0	2.5	0.33	0.187	0.189
95-#4–5 sand	0	95	0	5	0.33	0.176	0.212
92.5-#4–7.5 sand	0	92.5	0	7.5	0.33	0.160	0.231

correlation exists between the two measurement techniques. The differences between porosities calculated from the two methods could be due to the fact that the image analysis method determined the average accessible and inaccessible porosities based on the sections scanned (2-D), and not based on the entire volume of the sample (3-D) as in the case of the volumetric method.

3.3. Measurement of bulk resistance using electrical impedance spectroscopy

Several researchers have reported on the use of Electrical Impedance Spectroscopy (EIS) measurements in the study of cementitious materials [12–18]. EIS measurements were conducted in this study using a Solartron 1260™ Impedance/Gain-Phase analyzer that was interfaced with a personal computer for data acquisition. A typical Nyquist plot (plot of real versus imaginary impedance) obtained from EIS measurements consists of two arcs — the bulk arc and the electrode arc. The two arcs meet at a point where the imaginary component of the impedance is minimum, and the corresponding real impedance is the bulk resistance (R_b) of the sample.

Fig. 1a shows the specimen set up that was used for the experiments described in this paper. The cylindrical specimen was enclosed in a latex membrane to contain the electrolyte. The bottom of the specimen was sealed to a stainless steel plate using silicone sealant. After the specimen was saturated with the electrolyte, another stainless steel plate with a small acrylic dyke was placed at the top of the specimen, with a piece of porous foam in between to ensure proper electrical contact. The entire set up was firmly gripped with adjustable clamping mechanism. The stainless steel plates served as the electrodes and alligator plugs from the impedance analyzer were attached to the electrodes. The impedance measurements were made over the frequency range of 1 MHz to 10 Hz using a 250 mV AC signal.

Using the bulk resistance (R_b) obtained from the Nyquist plots, the effective electrical conductivity (σ_{eff}) of the sample was calculated as:

$$\sigma_{eff} = \frac{l}{R_b A} \quad (1)$$

where l is the specimen length and A is the cross sectional area of the specimen.

The values of σ_{eff} measured for the samples used in this study are given in Column 3 of Table 2. The electrolytes used in this study were sodium chloride (NaCl) solutions of varying concentrations (1%, 3%, and 10%). The conductivity of 1% NaCl solution was 1.56 S/m whereas the conductivities of 3% and 10% solutions were 4.40 S/m and 12.40 S/m respectively (Column 2 of Table 2).

3.4. Measurement of hydraulic conductivity

Since the EPC has a much higher hydraulic conductivity (of the order of 10^{-3} to 10^{-4} m/s, as compared to 10^{-12} m/s of normal concrete [19]) due the presence of large interconnected pore network, the conventional methods that are used to evaluate the hydraulic conductivity of normal concrete are not directly applicable. To estimate the hydraulic conductivity of EPC, a falling head permeability cell has been designed, as shown in Fig. 1b.

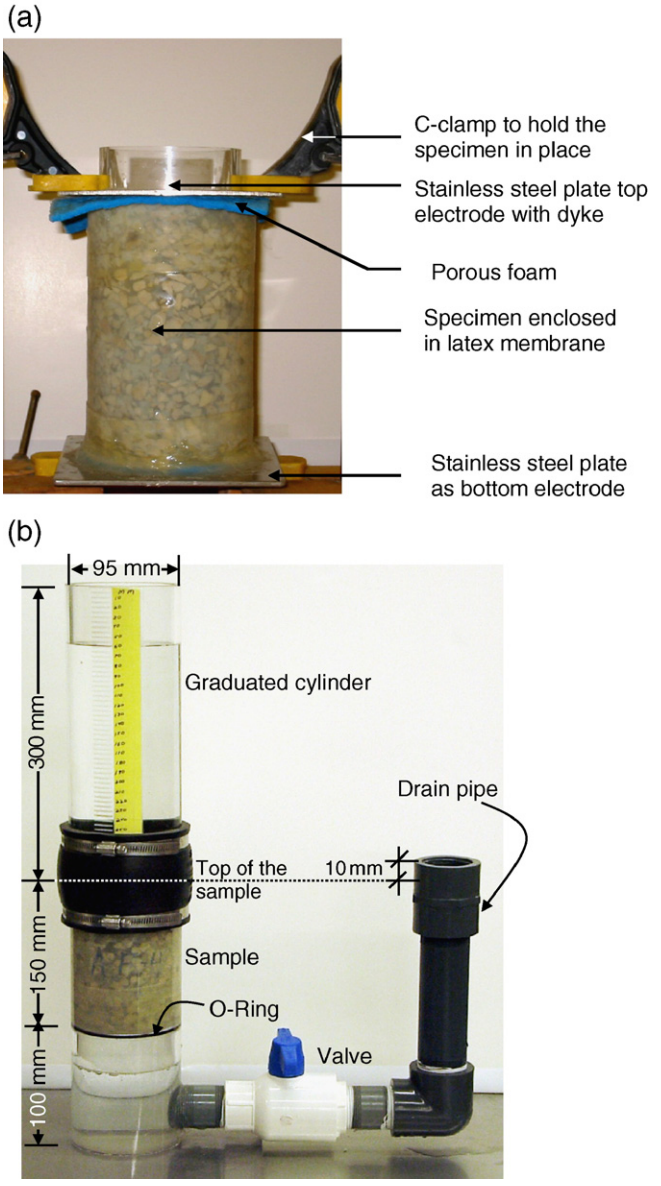

Fig. 1. (a) Specimen set up for electrical impedance measurements, (b) Falling head permeability cell to measure hydraulic conductivity.

The permeability cell consists of a 250 mm long acrylic tube with an inner diameter of 92 mm. The top 150 mm of the tube was machined to an inner diameter of 95 mm so that the specimen can be seated on an O-ring at a distance of 100 mm from the bottom. A 50 mm diameter valve connects the bottom part of the tube to a vertical pipe through which water can drain out. The top of this pipe is positioned 10 mm above the top of the specimen so that no unsaturated flow occurs during the test. A graduated acrylic cylinder of 300 mm length was attached to the top of the specimen assembly and clamped tightly using a

Table 2
Electrical, hydraulic, and acoustic properties of the EPC mixtures investigated

1	2	3	4	5	6	7	8	9
Mixture ID	Pore solution conductivity (S/m)	Measured conductivity (S/m)	Solid phase conductivity (S/m)	Predicted conductivity (modified Archie's law) (S/m)	Predicted conductivity (B–H equation) (S/m)	Pore connectivity factor (β_p)	Hydraulic connectivity factor (β_H)$\times 10^{-10}$	Maximum acoustic absorption coefficient (α)
100-#8	1.56	0.0369	0.0151	0.0429	0.0359	0.1078	4.567	0.61
	4.40	0.0936		0.0941	0.0872			
	12.40	0.2346		0.2384	0.2315			
75-#8–25-#4	1.56	0.0421	0.0168	0.0442	0.0364	0.1264	5.743	0.59
	4.40	0.1090		0.0946	0.0867			
	12.40	0.2388		0.2365	0.2286			
50-#8–50-#4	1.56	0.0464	0.0166	0.0559	0.0504	0.1266	7.2489	0.76
	4.40	0.1410		0.1281	0.1226			
	12.40	0.3281		0.3316	0.3261			
25-#8–75-#4	1.56	0.0579	0.0143	0.0758	0.0727	0.1797	12.731	0.81
	4.40	0.1888		0.1888	0.1857			
	12.40	0.4939		0.5071	0.5040			
100–#4	1.56	0.0346	0.0101	0.0432	0.0390	0.1080	5.833	0.61
	4.40	0.0965		0.1038	0.0996			
	12.40	0.2599		0.2746	0.2704			
75-#8–25-3/8	1.56	0.0324	0.0155	0.0347	0.0261	0.0746	5.456	0.42
	4.40	0.0626		0.0699	0.0613			
	12.40	0.1609		0.1691	0.1605			
50-#8–50-3/8	1.56	0.0280	0.0103	0.0242	0.0177	0.0799	3.325	0.28
	4.40	0.0636		0.0497	0.0432			
	12.40	0.1281		0.1216	0.1150			
25-#8–75-3/8	1.56	0.0087	0.0177	0.0267	0.0140	0.0542	5.955	0.56
	4.40	0.0765		0.0434	0.0432			
	12.40	0.0743		0.0902	0.0774			
100–3/8	1.56	0.0089	0.0095	0.0177	0.0107	0.0346	9.373	0.31
	4.40	0.0325		0.0327	0.0306			
	12.40	0.0689		0.0751	0.0681			
50-#4–50-3/8	1.56	0.0310	0.0173	0.0414	0.0334	0.0854	4.211	0.63
	4.40	0.0998		0.0856	0.0258			
	12.40	0.2065		0.2102	0.2023			
97.5–#4	1.56	0.0111	0.0027	0.0161	0.0144	0.0466	5.833	0.52
2.5 sand	4.40	0.0435		0.0406	0.0388			
	12.40	0.1066		0.1094	0.1077			
95–#4 7.5	1.56	0.0103	0.0018	0.0133	0.0118	0.0406	4.019	0.44
sand	4.40	0.0326		0.0343	0.0327			
	12.40	0.0914		0.0934	0.0919			
92.5–#4	1.56	0.0089	0.0022	0.0111	0.0095	0.0356	3.898	0.40
7.5 sand	4.40	0.0236		0.0272	0.0256			
	12.40	0.0700		0.0726	0.0710			

rubber sleeve. This was used to monitor the water level during the test.

The specimen was enclosed in a latex membrane (as was done for the electrical property measurements), and was inserted into the test set up. Water was added to the graduated cylinder to fill the specimen cell and the draining pipe. The specimen was pre-conditioned by allowing water to drain out through the pipe until the level in the graduated cylinder was the same as the top of the drain pipe. This eliminated any air pockets in the specimen and ensured that the specimen was completely saturated. With the valve closed, the graduated cylinder was filled with water. The valve was then opened, and the time in seconds (t) required for water to fall from an initial head of 290 mm (h_1) to a final head of 70 mm (h_2) measured. This procedure was repeated three times, and the average value of t was used.

The coefficient of permeability (K) was calculated according to Darcy's law as:

$$K = \frac{A_1 l}{A_2 l} \log\left(\frac{h_2}{h_1}\right) \tag{2a}$$

where A_1 and A_2 are the areas of the cross-section of the sample and the tube respectively and l is the length of the specimen. For a given specimen geometry, and same initial and final heads, the coefficient of permeability is given as:

$$K = \frac{A}{t} \tag{2b}$$

where A is a constant, which in this study was 0.084 m.

The measured values of hydraulic conductivity ranged from 0.001 to 0.005 m/s, with a standard deviation of 0.0003 to 0.0008 m/s (three repeated measurements).

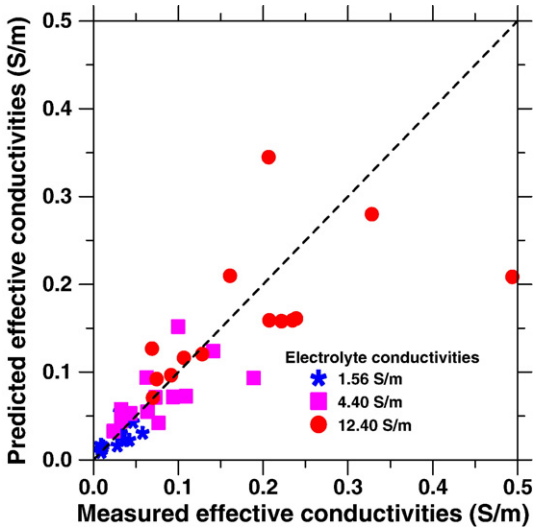

Fig. 2. Predicted effective conductivities from conventional Archie's law plotted against measured effective conductivities.

3.5. Measurement of acoustic absorption coefficient using impedance tube

Acoustic absorption coefficient (α) of a material is a measure of its ability to absorb sound. A perfectly absorbing material has a α value close to 1.0, whereas a perfectly reflecting material has a α value close to 0. Standard concrete mixtures have α values in the range of 0.05 to 0.10. The acoustic absorption coefficient of EPC was measured using a Brüel and Kjær™ impedance tube as per ASTM E 1050-98 [20]. The sample was placed in a thin cylindrical Teflon sleeve and the assembly was placed against a rigid backing at one end of the impedance tube. Microphones placed along the length of the tube were used to detect the sound pressure levels, which were then translated into the reflection and absorption coefficients. Further details about measurement and data analysis of these specimens can be found elsewhere [5,21]. The maximum absorption coefficients for the EPC mixtures are provided in Column 9 of Table 2.

4. Electrical conductivity studies

The effective electrical conductivity of a porous medium (σ_{eff}) with a conducting fluid phase depends on the electrical conductivities (σ_i), relative volumes (ϕ_i), and geometric distributions of each of the constituent phases. For a porous medium with a single conducting phase, Archie's law relates the overall conductivity of the material to that of a conducting medium present in the pores using Eq. (3) [8,22–28]:

$$\sigma_{\text{eff}} = C\sigma_0\phi_0^m \tag{3}$$

where C is a constant (typically assumed to be 1.0), σ_0 is the conductivity of the conducting medium, ϕ_0 is the pore volume fraction, and m is Archie's exponent. The exponent m depends on the geometry of constituent particles and their arrangement [27,29]. The values of m typically range from 1.5 to 4.0, with higher values indicating lower electrical connectivities of the phase [27,30].

4.1. Conductivity–porosity relations: single phase Archie's law

A plot of measured effective conductivities (σ_{eff}) and those predicted from Archie's law using Eq. (3) for the EPC mixtures is provided in Fig. 2. The m values were obtained from the fit of effective conductivity–porosity relationships for each electrolyte concentration. The three different symbols correspond to the three concentrations of the electrolyte used. As expected, the effective conductivity increases with the electrolyte conductivity. It can be observed that the agreement between the measured and predicted conductivities is rather poor, contrary to the behavior of saturated porous rock systems which show adherence to the single phase Archie's law with an m value of 1.5 to 2.5, the lower values being typically associated with smaller particle sizes [8,23–25,30], indicating that the conventional form of Archie's law may not be the best representation of the electrical behavior of EPC system.

To prove this point further, Nyquist plots of EPC specimens proportioned using single sized aggregates (#8, #4, and 3/8″) saturated with 3% NaCl electrolyte (conductivity 4.40 S/m) are shown in Fig. 3. Though the pore volumes of these mixtures fall in a very narrow range (0.19–0.21), a significant variation in the bulk resistances (or conductivities) exists. If Archie's law was to hold true, one would expect similar effective conductivities for these mixtures. The fair assumption in this case would be that the effective conductivity of the system is not only a function of the conductivity of the electrolyte in the pores and the porosity, but also on some other component in the material structure of EPC. It is hypothesized that the matrix that coats the aggregates is also conductive, as in conventional concrete mixtures. Therefore, the assumption of a single conducting phase is no longer completely valid.

4.2. Multi-phase conductivity models for EPC

Based on the aforementioned observation, it is expected that the effective conductivity of EPC may be better predicted by

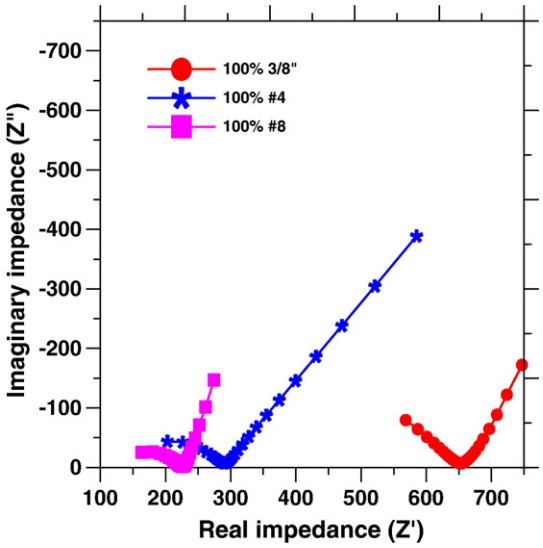

Fig. 3. Nyquist plots for EPC mixtures with single sized aggregates.

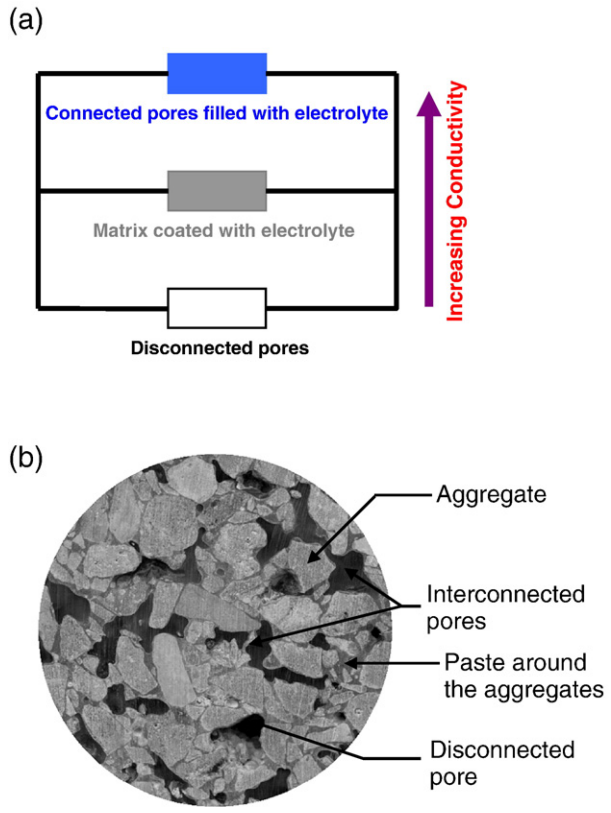

Fig. 4. (a) Dependence of conductivity on the different phases of EPC, (b) A section of EPC epoxy filled to distinguish the different pore phases.

considering the system to be a multi-phase medium, as illustrated in Fig. 4a. The interconnected pore network filled with the electrolyte is the phase with the highest conductivity, followed by the matrix that binds the aggregates, and the disconnected pores. For the case of EPC, interconnected pore network refers to the network of large sized pores deliberately incorporated into the material (by gap grading the aggregates) for better acoustic and hydraulic performance. It is assumed that the matrix that binds the aggregates is homogeneous and continuous. Fig. 4b shows an image of the EPC sample with these phases indicated.

Three alternative versions of multi-phase models are considered: (i) a modified version of Archie's law, (ii) an equation of the Bruggeman–Hanay type, and (iii) a modified parallel model.

4.2.1. Modified Archie's law

The conventional form of Archie's law does not account for a second conducting phase; therefore a modified version of Archie's law for multi-conducting phases [8] is adopted to represent the conductivity of EPC.

The EPC system is considered as consisting of two-phases – the first phase being the large open porosity filled with an electrolyte – called pore phase (volume fraction ϕ_p and conductivity σ_p), and the second, the solid phase (volume fraction ϕ_s and conductivity σ_s). The total volume of the material is equivalent to the sum of the pore and solid fractions:

$$\phi_p + \phi_s = 1 \tag{4}$$

Using this approach, the modified Archie's law for a two-phase system takes the form [23]:

$$\sigma_{eff} = \sigma_p \phi_p^m + \sigma_s \phi_s^{m'} \tag{5}$$

where σ_p is the conductivity of the electrolyte in the pores, and σ_s is the conductivity of solid phase (in a water saturated condition). The exponents m and m' represent the degree of connectivity of the pore and solid phases respectively; a lower value indicating better connectivity [8]. For a material with low connectivity of the pore phase and very high connectivity of the solid phase (as in porous rocks, and concrete), $m > 1$, and $m' << 1$. The conductivity of the solid phase is derived from the fact that the conductive matrix that binds the aggregates is continuous (connectivity factor close to 1.0).

The effective conductivity of the composite (Table 2), and the volume fraction of the pores (Table 1) can be directly measured. Once the pore volume fraction is known, the volume of solids (ϕ_s) can be obtained from Eq. (4). The conductivity of the electrolyte can be easily controlled. Therefore, the conductivity of the solid phase (σ_s), and the exponents m and m' are the only unknowns. Assuming that the conductivity of the solid phase and the exponents representing the degree of connectivity will remain constant for a particular mixture, three different electrolyte conductivities (σ_p) were used and the corresponding effective conductivities (σ_{eff}) were measured. The tests were conducted in the order of the increasing ionic strength of the electrolytes so as to minimize any chances of σ_s being affected by the changing σ_p. This results in three variants of Eq. (5), which can be solved simultaneously to obtain the values of σ_s, m and m'. The values of σ_s are given in Column 4 of Table 2. It can be noticed from Table 2 that σ_s remains almost the same (~0.01 S/m for EPC matrices with no sand and ~0.002 S/m for matrices with sand) with varying electrolyte conductivity for various mixtures investigated. This is consistent with the idea that σ_s is necessarily a property of the "solid" matrix.

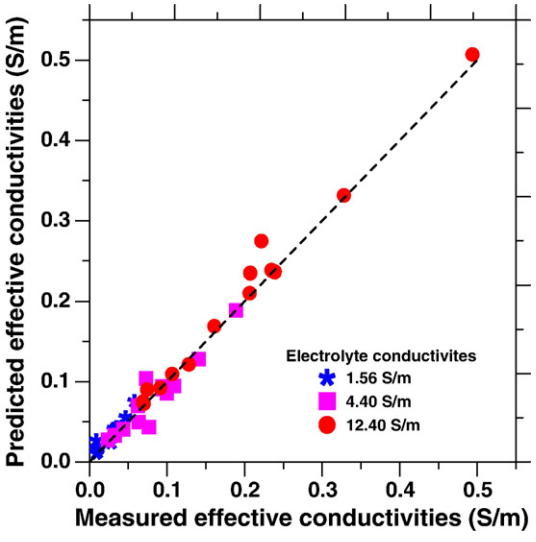

Fig. 5. Predicted effective conductivities from modified Archie's law plotted against measured effective conductivities.

The relationship between the measured electrical conductivities and those predicted by modified Archie's law for all three electrolyte conductivities is shown in Fig. 5. On comparison with Fig. 2, it is immediately evident that the predictive capability is improved by modifying Archie's law (the average deviation between the measured conductivities and those predicted by modified Archie's law is around 7%, whereas it is around 35% for conventional Archie's law). It also validates the assumption that the conductivity of EPC is dependent on more than just the characteristics of the pore phase alone.

It was also found from the solution of simultaneous equations to obtain σ_s, m and m', that the term m' is very small (0.03–0.10), rendering the value of $\phi_s^{m'}$ close to 1.0. Similar values of m' have been reported in the literature for materials analogous to saturated porous rocks [8]. Hence, the modified Archie's law can be simplified to:

$$\sigma_{eff} = \sigma_p \phi_p^m + \sigma_s \tag{6}$$

Since σ_s is a constant irrespective of the conductivity of the electrolyte, the effective conductivity becomes less and less dependent on the matrix conductivity as the electrolyte conductivity is increased.

4.2.2. Bruggeman–Hanay approach

The Bruggeman–Hanay equation [23] has been used to relate the electrical properties of a heterogeneous mixture to the properties of individual components. For a granular material composed of conductive homogeneous particles of conductivity σ_s embedded in a medium of conductivity σ_p, the composite electrical conductivity σ_{eff} is given by:

$$\sigma_{eff} = \sigma_p \phi_p^m \left[\frac{1-\frac{\sigma_s}{\sigma_p}}{1-\frac{\sigma_s}{\sigma_{eff}}}\right]^m \tag{7}$$

where ϕ_p is the porosity and m is originally defined as a non-dimensional parameter that depends on the aspect ratio of the grains (equivalent to the Archie's exponent m). When $\sigma_s \to 0$, Eq. (7) reduces to Archie's law for a single conducting medium.

Assuming that conductivity of the composite is dominated by the pore fluid ($\sigma_p >> \sigma_s$), the equation can be simplified by a binomial expansion and retaining the first-order terms [23,30] resulting in Eq. (8):

$$\sigma_{eff} \approx \phi_p^m [\sigma_p + m(\phi_p^{-m} - 1)\sigma_s] \tag{8}$$

The advantage of such a relation as compared to the modified Archie's relation discussed in the previous section is that this equation contains only two unknowns (σ_s and m) as compared to three (σ_s, m and m') of modified Archie's equation.

The effective conductivities predicted from Eq. (8) are given in Column 6 of Table 2, and plotted against the measured values in Fig. 6 for all three electrolyte conductivities chosen for the study. The measured conductivities and those predicted using Bruggeman–Hanay equation are in good agreement (differing on an average by about 9%), reiterating the significance of incorporating the matrix conductivity in effective conductivity predictions.

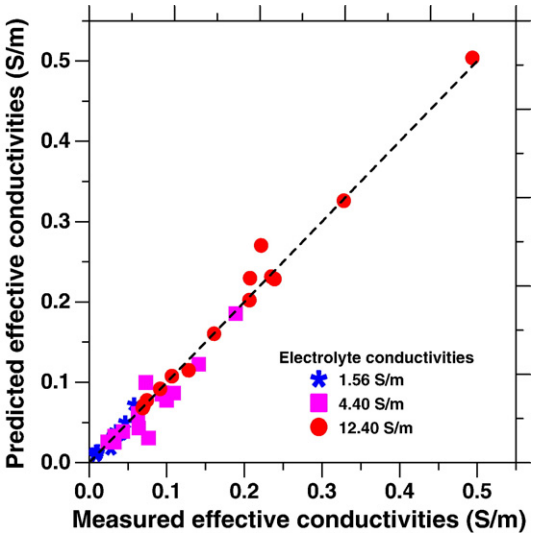

Fig. 6. Predicted effective conductivities from Bruggeman–Hanay equation plotted against measured effective conductivities.

4.2.3. Modified parallel model

The complex distributions of pore and solid phases in a porous material with different volume fractions of constituents and conductivities differing by orders of magnitude have been approximated by simpler models [8,13,23]. One such model is the parallel model where the effective conductivity is given by the arithmetic mean of the conductivities of each phase weighted by their respective volume fractions, as expressed by Eq. (9).

$$\sigma_{eff} = \sigma_p \phi_p + \sigma_s \phi_s \tag{9}$$

where σ_{eff}, σ_p, σ_s, ϕ_p, and ϕ_s are the same as described in Section 4.2.1.

The first element represents the conductivity associated with the free electrolyte in the larger pores of EPC while the other represents the conductivity associated with the matrix that binds the aggregates. The drawback of such a model is that this representation does not take into account the connectivity of the pore and the solid networks. To counter this, the parallel model has been modified by including a connectivity factor (β) [31]. The modified parallel model then becomes:

$$\sigma_{eff} = \sigma_p \phi_p \beta_p + \sigma_s \phi_s \beta_s \tag{10}$$

where β_p and β_s are termed the connectivity factors, representing the connectivities of the pore and the solid phases respectively, much like the exponents m and m' in the modified Archie's law. The only difference between the exponents and the connectivity factors is that higher exponents imply decreased connectivity whereas an increase in the β factor implies increased connectivity. A term, modified normalized conductivity $\left(\frac{\sigma_{eff} - \sigma_s \phi_s}{\sigma_p}\right)$ is defined (hereinafter expressed as σ_{norm}*), which can be thought of as a true measure of the pore structure of the material. The numerator is taken as $(\sigma_{eff} - \sigma_s \phi_s)$ since the

solid connectivity factor β_s in Eq. (10) could be safely approximated to be equal to unity. Eq. (10) then becomes

$$\sigma_{eff} = \sigma_p \phi_p \beta_p + \sigma_s \phi_s \tag{11}$$

From Eq. (11), the pore phase connectivity (β_p) is given by:

$$\beta_p = \frac{(\sigma_{eff} - \sigma_s \phi_s)}{\sigma_p} \frac{1}{\phi_p} = \frac{\sigma^*_{norm}}{\phi_p} \tag{12}$$

The pore connectivity factors for the EPC mixtures studied are given in Column 7 of Table 2.

4.2.4. Relationship between β_p and m

Equating the modified form of Archie's law Eq. (6) and the modified parallel law Eq. (11),

$$\sigma_p \phi_p^m + \sigma_s = \sigma_p \phi_p \beta_p + \sigma_s \phi_s \tag{13a}$$

Rearranging the terms, and simplifying,

$$\sigma_p \phi_p (\beta_p - \phi_p^{m-1}) = \sigma_s (1 - \phi_s) \tag{13b}$$

$$\left(\beta_p - \phi_p^{m-1}\right) = \frac{\sigma_s}{\sigma_p} \tag{13c}$$

The pore phase conductivity is much higher than solid phase conductivity — $\sigma_p >> \sigma_s$ (of the order of two magnitudes or more), and hence $\left[\frac{\sigma_s}{\sigma_p}\right] \rightarrow 0$.

Hence, the pore connectivity factor can be expressed as:

$$\beta_p = \phi_p^{m-1} \tag{13d}$$

This equation gives a straightforward calculation of pore connectivity factor based on the pore volume fraction and the exponent m from modified Archie's law. Eq. (12) provides a value of β_p from the measured conductivities whereas Eq. (13d) is a derived value. The agreement between the calculated β_p from both Eqs. (12) and (13d) is shown in Fig. 7, indicating the validity of the exponent m calculated from modified Archie's law. This relationship also shows that Archie's exponent m can be used as a measure of the pore connectivity.

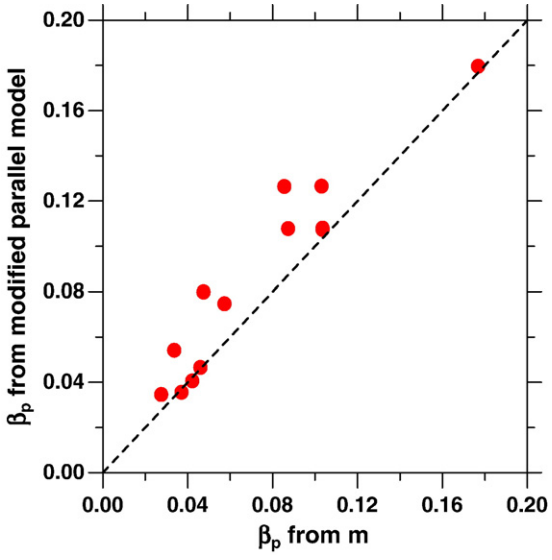

Fig. 7. Relationship between pore connectivity factors calculated from modified Archie's exponent as well as from modified parallel model.

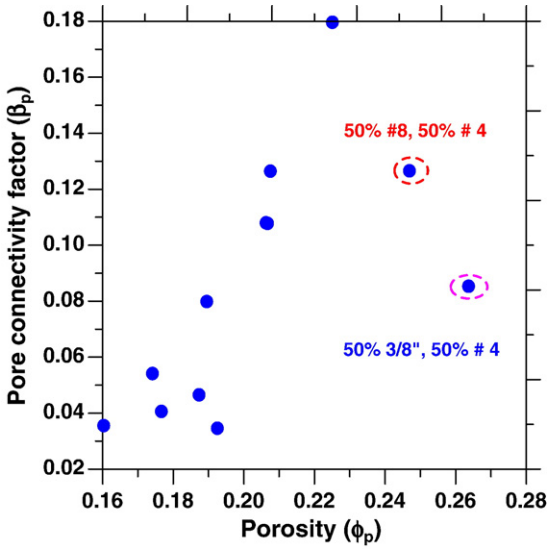

Fig. 8. Relationship between porosity and pore connectivity factor calculated from the modified parallel model.

4.2.5. Comparison between the multi-phase models

The first two multi-phase models presented above are variants of the Archie's law, where the connectivity of the constituent phases are represented by the exponents. Modified Archie's law and Bruggeman–Hanay equation were found to deviate from the measured conductivities by 7% and 9% respectively, and as such there is no real reason to choose one model over the other. One advantage with using the Bruggeman–Hanay equation is that there are only two unknowns involved, therefore the use of electrolyte with two different concentrations is sufficient. The modified parallel model uses a multiplicative connectivity factor (β), an increase in which implies increased connectivity of the corresponding phase. Due to the simplicity of the modified parallel model, it will be used further in this paper for assessing the acoustic performance and the prediction of hydraulic conductivity of EPC mixtures.

4.3. Porosity and pore connectivity factor

The relationship between the porosity (ϕ_p) and the pore phase connectivity factor (β_p) is shown in Fig. 8. The plot shows that even when the pore volume fraction is similar, the pore connectivity can be quite different. Though the connectivity factor should increase with porosity, it can be noticed that there exists substantial scatter in the results. However, this behavior is not observed for all values of porosity. The data points that show a deviation from this trend are those containing 50% #4 aggregates with either 50% 3/8″ or 50% #8 aggregates. The blends in both these cases are such that the smaller sized

aggregates are not able to fill in the pore spaces between the larger sized aggregate [5], resulting in a higher overall porosity. Because of the arrangement of the particles, the connectivity factor of these mixtures is lower than some of the mixtures that have a lower porosity. This is further validated using acoustic absorption measurements in the following section.

4.4. Pore connectivity and its relation to acoustic absorption

The acoustic absorption of EPC is related to the porosity, pore size, pore connectivity, and the constrictions in the pore network through which acoustic energy can travel and attenuate inside the material. The acoustic absorption coefficient (α) is a measure of the ability of the material to absorb sound. Acoustic absorption spectra (variation of absorption coefficient with frequency) for various EPC mixtures were generated following the procedure described in Section 3.5. Typical acoustic absorption spectra for these materials can be found elsewhere [5].

It has been explained in Section 4.3 that even when the pore volume fraction is the same, its connectivity can be different, and it significantly influences the conductivity as well as the acoustic absorption coefficient. Thus, pore connectivity is an important pore feature that takes into account the constrictions in the pore space, which can be used to characterize the efficiency of EPC with respect to acoustic absorption. The relation between pore connectivity factor (β_p) and maximum acoustic absorption coefficient (α) for various EPC mixtures investigated in this study is shown in Fig. 9. The maximum absorption coefficient increases with increasing pore connectivity and the relationship is relatively linear ($R^2=0.81$).

The preceding discussion focused on extracting the pore structure features of EPC from electrical conductivity measurements. The need for a multi-phase conductivity model has been brought out, and the relationships between porosity, pore connectivity, and electrical conductivity has been arrived at. From these, it is evident that a combination of pore structure features – porosity that can be directly measured, and pore connectivity factor determined through electrical conductivity experiments – form a powerful tool to characterize the pore structure of EPC and ascertain its efficiency in acoustic absorption.

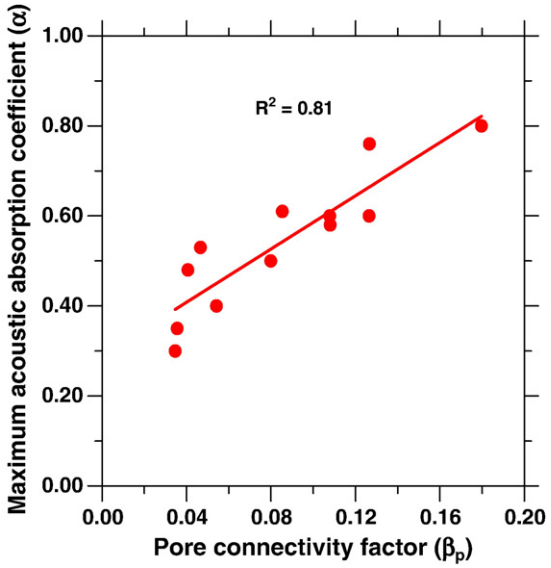

Fig. 9. Relationship between pore connectivity factor and maximum acoustic absorption coefficient.

5. Hydraulic conductivity studies

The hydraulic conductivity (K) of a porous material is determined by the arrangement of particles, pores, and their relative sizes. The intrinsic permeability (k) of a porous medium can be thought of as a measure of the frictional resistance to a fluid flowing through it. Therefore, the intrinsic permeability depends on the porosity, pore-size distribution, pore roughness, constrictions of the pore space, and the tortuosity and connectivity of the internal pore channels [28]. The hydraulic conductivity can be related to intrinsic permeability as:

$$K = k\frac{\rho g}{\mu} \tag{14a}$$

where ρ is the density of the fluid, g is the acceleration due to gravity, and μ is the dynamic viscosity of the fluid. For water, this equation can be simplified as:

$$K = k * 10^7 \text{ (in SI units)} \tag{14b}$$

The intrinsic permeability of porous media is typically described using the Kozeny–Carman equation:

$$k = \frac{\phi_p^3}{F_s \tau^2 S_0^2 (1-\phi_p)^2} \tag{15}$$

where ϕ_p is the porosity, F_s is the generalized factor to account for different pore shapes, τ is the tortuosity, and S_0 is the specific surface area of pores.

5.1. Relationship between porosity and intrinsic permeability

Several studies have predicted the permeability (permeability in this paper refers to intrinsic permeability) of porous media from the porosity. For example, it has been suggested that Darcy's law could be given a form similar to Archie's law [28], to relate the permeability and porosity of rock systems:

$$k = a_1 \phi^{b_1} \tag{16}$$

where k is the intrinsic permeability (units of m^2), ϕ is the porosity, and a_1 and b_1 are constants. However, the predicted and measured permeabilities in this study were not observed to correlate well since permeability is not a function of the porosity alone, rather connectivity and porosity are critical in understanding the permeability of the system.

For the EPC mixtures investigated in this study, the porosity–permeability relationship is shown in Fig. 10. While permeability generally increases with an increase in porosity, there is no definitive relationship between these parameters. The reason for such poor correlation can be explained by the fact that porosity is a volumetric property of the material, whereas permeability is a parameter that defines the flow properties through the material that not only depends on the volume of the pores but also on the distribution of the pore volume and its connectivity. In that sense, it is similar to the electrical conductivity, which was shown in the previous sections to have a dependence on the pore connectivity in addition to the porosity.

5.2. Pore structure features and permeability

The relationship between porosity and permeability is given by the Kozeny–Carman relation Eq. (15). It can be shown that the tortuosity (τ) is equivalent to the inverse of connectivity ($\tau = 1/\beta_p$).

It can be seen from Eq. (12) that $\beta_p \phi_p$ is equivalent to σ^*_{norm}. Therefore, the term $[\frac{\phi_p}{\tau}]^2$ in Kozeny–Carman equation is equivalent to, and can be replaced by $[\sigma^*_{norm}]^2$.

Using this approach, Kozeny–Carman equation can be rewritten as:

$$k = \frac{1}{F_s S_0^2}[\sigma^*_{norm}]^2 \left(\frac{\phi_p}{(1-\phi_p)^2}\right) \quad (17)$$

This illustrates that the intrinsic permeability (k) is equal to the product of a constant that describes the shape and specific surface area of pores, the square of modified normalized conductivity, and a function that accounts for the pore volume fraction.

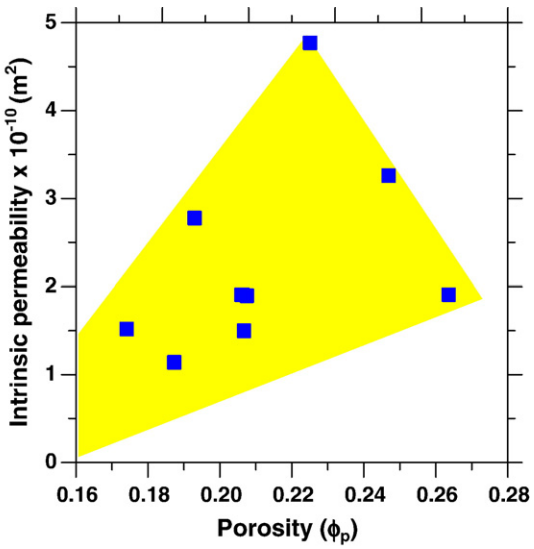

Fig. 10. Porosity–permeability relationship.

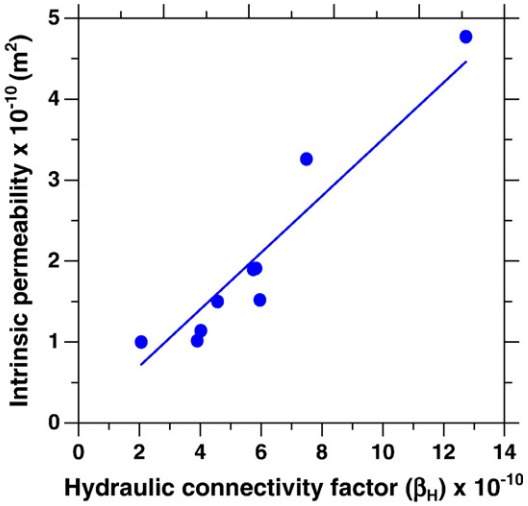

Fig. 11. Intrinsic permeability (k) versus hydraulic connectivity factor (β_H).

The expression $\frac{1}{F_s S_0^2}[\sigma^*_{norm}]^2$ is defined as the *hydraulic connectivity factor* (β_H). Column 8 of Table 2 gives the values of β_H for the specimens studied. The Kozeny–Carman equation can then be simplified as:

$$k = \beta_H \left(\frac{\phi_p}{(1-\phi_p)^2}\right) \quad (18)$$

The intrinsic permeability therefore is represented as a function of porosity (ϕ_p), and the hydraulic connectivity factor (β_H). The hydraulic connectivity factor (β_H) can be thought of as a combination of parameters that describe the pore space volume and geometry in such a way that the intrinsic permeability is related to porosity and hydraulic connectivity factor. The relationship between k and β_H is shown in Fig. 11.

The hydraulic connectivity factor β_H offers a means of classifying EPC based on their hydraulic characteristics. The mixtures with similar β_H values exhibit similar permeability (k). The mixture with a low β_H value (i.e., 100% #8 aggregates) has a small aggregate size. Therefore, the inter-particle pore sizes are also small and as a result its ability to sustain water flow is lower. Similarly, the mixture with 50% #8 and 50% 3/8″ aggregates also has a low β_H value since the smaller aggregates fill in between the larger particles, resulting in a reduced porosity and a reduced flow capacity. The mixtures with the highest β_H values either have a large porosity and pore size as with mixtures having 100% 3/8″ aggregates or has a blend of aggregate sizes that helps to create a very continuous pore structure, as in mixtures with 75% #4 and 25% #8 aggregates.

5.3. Acoustic absorption and intrinsic permeability

Examining the hydraulic connectivity factor (β_H) and the maximum acoustic absorption (α) values (Table 2), it is rather difficult to obtain a direct relationship between the acoustic absorption and intrinsic permeability (recall $k \propto \beta_H$). For instance, the mixture with 100% 3/8″ aggregates exhibited the lowest

acoustic absorption characteristics, but has a higher permeability. The reason for this behavior can be described as follows: when the material has very large sized pores and fairly large apertures to connect the pores (i.e., lesser pore constrictions), the drainage of water will be rapid and the permeability will be high. But sound waves can easily pass through these large pores without losing much energy because the pore structure does not force them to alternatively compress and expand, consequently resulting in a lower acoustic absorption. The mixture with 100% #8 aggregates, on the other hand, has a lower pore size and is hydraulically inefficient, resulting in a lower β_H value. But the ratio of pore and aperture sizes for this mixture is in the acoustically efficient range, resulting in a higher acoustic absorption coefficient. Alternatively, there are instances of aggregate blends like 75% #4 and 25% #8 where the pore and aperture sizes created by the aggregate blending are very effective in increasing permeability as well as acoustic absorption. This is an evidence of the fact that there exists an optimal range of pore sizes and connectivity that make the material both hydraulically and acoustically efficient.

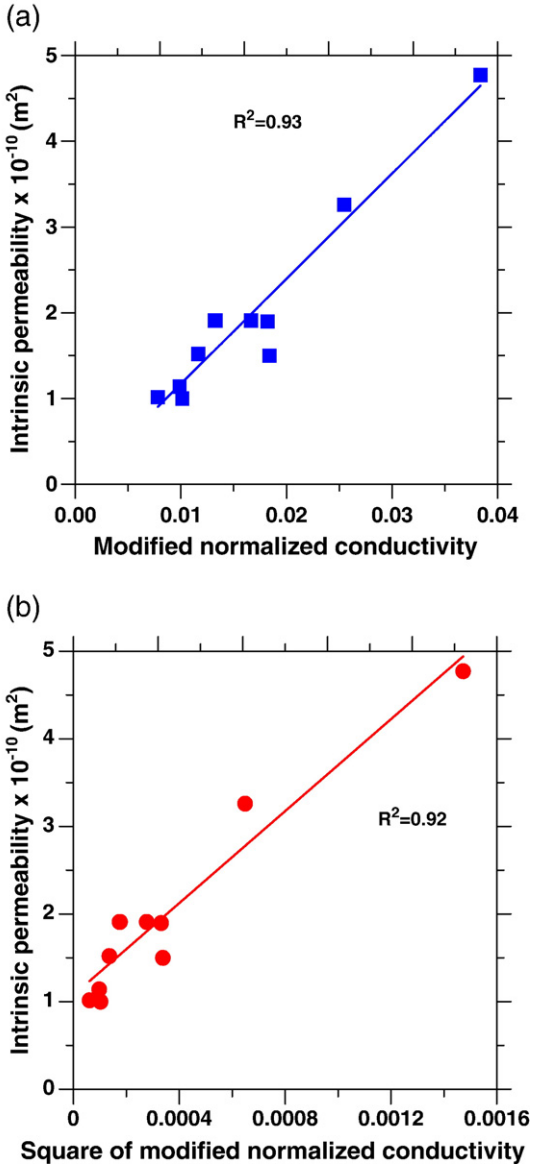

Fig. 12. Relationship between (a) intrinsic permeability and modified normalized conductivity $[\sigma^*_{norm}]$, and (b) square of modified normalized conductivity $[\sigma^*_{norm}]^2$.

5.4. Relating electrical conductivity and permeability

The final stage of this work was to relate the electrical conductivity with the intrinsic permeability of EPC. Eq. (17) showed that the intrinsic permeability could be related to the square of the modified normalized conductivity. This is similar to the findings of Wong et al. 1984 [24]. It should however be noted that some authors [32] have expressed the intrinsic permeability as:

$$k = \beta' \phi_p l_c^2 \tag{19}$$

where β' is a factor that accounts for the tortuosity (or connectivity) of the pores (similar to β_p), and l_c is a characteristic length.

Eq. (19) can be rewritten using normalized conductivity (by substituting Eq. (12) into (19)), to yield Eq. (20).

$$k = \left[\sigma^*_{norm}\right] \frac{\beta'}{\beta_p} l_c^2 \tag{20}$$

From this equation, it can be seen that permeability could be considered as being directly proportional to the modified normalized conductivity.

As some authors relate permeability to the normalized conductivity [32,33] while others relate permeability to the square of the normalized conductivity [[24], Eq. (17)], the modified normalized electrical conductivity, as well as its square are plotted against the intrinsic permeability in Fig. 12a and b respectively. The plots show that there is no significant statistical difference between the two (R^2 values of 0.93 and 0.92, respectively), but as Eq. (17) can be easily derived from the Kozeny–Carman equation, it is recommended that the permeability of EPC should be taken as being related to the square of the electrical conductivity.

6. Conclusions

This paper uses electrical impedance measurements to assess the pore structure of EPC for use in hydraulic and acoustic property characterization. The study consisted of measuring the electrical conductivity, hydraulic conductivity, and acoustic absorption of various EPC mixtures. The conclusions from this study are summarized as follows:

1. A single conducting phase model (i.e., like Archie's law) showed a 35% average error in predicting the effective conductivity of EPC. To improve the accuracy of the prediction, models that incorporate two conducting phases were evaluated (a modified version of Archie's law, an equation of the Bruggeman–Hanay type, and a modified parallel law). These two conducting phase models were found to adequately describe the electrical conductivity of EPC system, with similar values of average errors of 7–10%.
2. The pore connectivity factor (β_p) and the maximum acoustic absorption coefficient (α) were found to be linearly related. By using the pore connectivity factor (β_p) determined through electrical conductivity experiments, the pore structure of EPC

could be characterized and its efficiency in acoustic absorption can be ascertained.

3. Individually, porosity and electrical conductivity are inadequate descriptors of the hydraulic flow characteristics of the EPC system. The Kozeny–Carman equation has been modified to enable a hydraulic connectivity factor (β_H) to be obtained, which is observed to be proportional to the product of the square of the modified normalized electrical conductivity and a function of porosity. Therefore β_H can be used as an index to classify the EPC systems. Mixtures having similar values of hydraulic connectivity factor (β_H) exhibit similar permeabilities irrespective of their porosities.
4. The pore features that result in efficient hydraulic and acoustic performance differ. The normalized electrical conductivity can be used to obtain the pore connectivity (Eq. (12)), which provides a measure of the acoustic effectiveness of the material. The product of electrical conductivity and a function of the total porosity describe the intrinsic hydraulic permeability (Eq. (17)). The reason for this difference lies in the fact that the features of an acoustically efficient material (smaller pore sizes, and high pore constriction) are not the same as a hydraulically efficient material (open porosity, large pore sizes, and low pore constriction). Though these two parameters may seem to be inversely related, it was found that there are certain mixtures (blended aggregates) in which the effective pore sizes and pore connectivity created by blending the aggregates result in a system that can be made effective for both acoustic and hydraulic performance.

Acknowledgements

The authors gratefully acknowledge the support received from the Institute for Safe, Quiet, and Durable Highways (SQDH) and the Center for Advanced Cement Based Materials (ACBM). The second author also gratefully acknowledges support from the NSF Grant No. 0034272, a CAREER Grant. This work was conducted in the Charles Pankow Concrete Materials Laboratory; as such the authors gratefully acknowledge the support that has made this laboratory possible.

References

[1] Surface properties of concrete roads in accordance with traffic safety and reduction of noise, BRITE/EURAM Project BE 3415, November 1994.
[2] Traffic noises and road surfaces: State of the art, SIRRUS project, Belgian Road Research Center, Brussels, March 2000.
[3] P.M. Nelson, S.M. Phillips, Quieter road surfaces, TRL Annual Review, Transportation Research Laboratories, UK, 1994.
[4] E. Onstenk, A. Aguado, E. Eickschen, A. Josa, Laboratory study of porous concrete for its use as top layer of concrete pavements, Proceedings of the Fifth International Conference on Concrete Pavement and Rehabilitation, Purdue University, Indiana, vol. 2, 1993, pp. 125–139.
[5] A. Marolf, N. Neithalath, E. Sell, W.J. Weiss, J. Olek, Influence of aggregate size and gradation on the acoustic absorption of Enhanced Porosity Concrete, ACI Mater. J 101 (1) (2004) 82–91.
[6] B. Gerharz, Pavements on the base of polymer-modified drainage concrete, Colloids Surf., A Physicochem. Eng. Asp. 152 (1999) 205–209.
[7] J. Yang, G. Jiang, Experimental study on properties of pervious concrete pavement materials, Cem. Concr. Res. 33 (2003) 381–386.
[8] P.W.J. Glover, M.J. Hole, J. Pous, A modified Archie's law for two conducting phases, Earth Planet. Sci. Lett. 180 (2000) 369–383.
[9] R.W. Vervoot, S.R. Cattle, Linking hydraulic conductivity and tortuosity parameters to pore space geometry and pore-size distribution, J. Hydrol. 272 (2000) 36–49.
[10] J. Bear, Dynamics of Fluids in Porous Media, Elsevier, New York, 1972.
[11] ASTM C 192-00, Standard Method of Making and Curing Concrete Test Specimens in the Laboratory, American Society of Testing and Materials, Pennsylvania, 2000.
[12] P. Gu, Z. Xu, P. Xie, J.J. Beaudoin, Application of A.C. impedance techniques in studies of porous cementitious materials — (I) Influence of solid phase and pore solution on high frequency resistance, Cem. Concr. Res. 23 (1993) 531–540.
[13] B.J. Christensen, R.T. Coverdale, R.A. Olson, S.J. Ford, E.J. Garboczi, H.M. Jennings, T.O. Mason, Impedance spectroscopy of hydrating cement based materials: measurement, interpretation and application, J. Am. Ceram. Soc. 77 (1994) 2789–2804.
[14] S.J. Ford, T.O. Mason, B.J. Christensen, R.T. Coverdale, H.M. Jennings, Electrode configurations and impedance spectra of cement pastes, J. Mater. Sci. 30 (1995) 1217–1224.
[15] R.T. Coverdale, B.J. Christensen, H.M. Jennings, T.O. Mason, D.P. Bentz, E.J. Garboczi, Interpretation of impedance spectroscopy via computer modeling — Part I. Bulk conductivity and offset resistance, J. Mater. Sci. 30 (1995) 71–719.
[16] G.M. Moss, B.J. Christensen, T.O. Mason, H.M. Jennings, Microstructural analysis of young cement pastes using impedance spectroscopy during pore solution exchange, Adv. Cem. Based Mater. 4 (1996) 68–75.
[17] K.A. Synder, C. Ferraris, N.S. Martys, E.J. Garboczi, Using impedance spectroscopy to assess the viability of rapid chloride test for determining chloride conductivity, J. Res. Natl. Inst. Stand. Technol. 105 (4) (2000) 497–509.
[18] W.J. McCarter, G. Starrs, T.M. Chrisp, Electrical conductivity, diffusion, and permeability of Portland cement-based mortars, Cem. Concr. Res. 30 (2000) 1395–1400.
[19] A.M. Neville, Properties of Concrete, Addison Wesley Longman Limited, Essex, England, 1996.
[20] ASTM E 1050-98, Standard Test Method for Impedance and Absorption of Acoustic Materials using a Tube, Two Microphones and a Digital Frequency Analysis System, American Society of Testing and Materials, Pennsylvania, 1998.
[21] N. Neithalath, W.J. Weiss, J. Olek, Acoustic performance and damping behavior of cellulose-cement composites, Cem. Concr. Compos. 26 (2004) 359–370.
[22] H.W. Whittington, J. McCarter, M.C. Forde, The conduction of electricity through concrete, Mag. Concr. Res. 33 (114) (1981) 48–60.
[23] A.E. Bussian, Electrical conductance in a porous medium, Geophysics 48 (9) (1983) 1258–1268.
[24] P. Wong, J. Koplik, J.P. Tomanic, Conductivity and permeability of rocks, Phys. Rev., B 30 (11) (1984) 6606–6614.
[25] J.N. Roberts, L.M. Schwartz, Grain consolidation and electrical conductivity in porous media, Phys. Rev., B 31 (9) (1985) 5990–5997.
[26] B.J. Christensen, Microstructure studies of hydrating Portland cement based materials using impedance spectroscopy, PhD Thesis, Northwestern University, 1993.
[27] P.D. Chinh, Electrical properties of sedimentary rocks having interconnected water-saturated pore spaces, Geophysics 65 (4) (2000) 1093–1097.
[28] O.A.L. de Lima, Sri Niwas, Estimation of hydraulic parameters of shaly sandstone aquifers from geoelectrical measurements, J. Hydrol. 235 (2000) 12–26.
[29] P.D. Jackson, D.T. Smith, P.N. Stanford, Resistivity–porosity–particle shape relationships for marine sands, Geophysics 43 (6) (1978) 1250–1268.
[30] O.A.L. de Lima, M.M. Sharma, A grain conductivity approach to shaly sandstones, Geophysics 55 (10) (1990) 1347–1356.
[31] E.J. Garboczi, Permeability, diffusivity and microstructural parameters: a critical review, Cem. Concr. Res. 20 (1990) 591–601.
[32] N. Martys, E.J. Garboczi, Length scales relating to the fluid permeability and electrical conductivity in random two-dimensional model porous media, Phys. Rev., B 46 (10) (1992) 6080–6090.
[33] A.J. Katz, A.H. Thompson, Quantitative prediction of permeability in porous rock, Phys. Rev., B 34 (11) (1986) 8179–8181.